Potential-Modulated Attenuated Total Reflectance Characterization of Charge Injection Processes in Monolayer-Tethered CdSe Nanocrystals

ARTICLE *in* JOURNAL OF PHYSICAL CHEMISTRY LETTERS · JUNE 2010

Impact Factor: 7.46 · DOI: 10.1021/jz100475j

4 AUTHORS, INCLUDING:

R. Clayton Shallcross
The University of Arizona
17 PUBLICATIONS **217** CITATIONS

SEE PROFILE

THE JOURNAL OF PHYSICAL CHEMISTRY Letters

pubs.acs.org/JPCL

Potential-Modulated Attenuated Total Reflectance Characterization of Charge Injection Processes in Monolayer-Tethered CdSe Nanocrystals

Zeynep Ozkan Araci, Clayton R. Shallcross,† Neal R. Armstrong,* and S. Scott Saavedra*

Department of Chemistry and Biochemistry, University of Arizona, Tucson, Arizona, 85721-0041

ABSTRACT Reversible electron injection into pyridine-capped CdSe nanocrystals (pyr-CdSe NCs), tethered to indium−tin oxide (ITO) substrates using mercaptoalkylcarboxylic acids, is characterized using attenuated total reflectance (ATR) spectroelectrochemistry on a planar waveguide. The sensitivity of this technique provides for characterization of redox processes in submonolayer films of pyr-CdSe NCs. Optically determined onset potentials for electron injection, measured as bleaching/recovery of the exciton absorption band, provide estimates for the conduction band edge (E_{CB}). Potential-modulated attenuated total reflectance (PM-ATR), in which the in-phase and out-of-phase reflectance response is measured as a function of modulation frequency, provides estimates for rates of electron injection. These apparent rate constants are found to be nearly independent of tether chain length, suggesting that communication between tethered NCs and electrochemically less active (i.e., less conductive) regions on the ITO surface is rate-limiting.

SECTION Electron Transport, Optical and Electronic Devices, Hard Matter

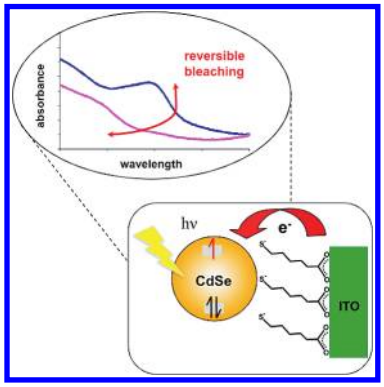

Semiconductor nanocrystalline materials are of interest as photocatalysts for the formation of solar fuels,[1−6] as sensitizers for dye-sensitized solar cells based on nanoporous metal oxides,[3,7−9] as luminescent dopants in light emitting diodes,[10,11] and as light-absorbing, electron transporting materials in solar cells.[12−14] Rates of photoactivated electron and hole transfer for nanocrystals (NCs) depend on frontier orbital energies (conduction and valence band edges, E_{CB} and E_{VB}, respectively), which are strongly dependent on NC size and composition, capping ligand, and the dielectric properties of the surrounding environment (vacuum vs electrolyte solutions vs polymer hosts).[1−5,15−22]

Conventional voltammetric techniques, sometimes coupled with characterization of electrogenerated chemiluminescence (ECL) in solutions of ligand-capped CdSe, CdSe and CdTe NCs, have been used to estimate onset potentials for oxidation/reduction, from which E_{VB}, E_{CB}, and "quasi-particle energy gaps" can be estimated.[15−17] These oxidation and reduction events can be difficult to resolve from background currents and are chemically irreversible on normal voltammetric time scales. The ECL response of CdSe NCs, however, suggests that the charged states of these ligand-capped NCs are sufficiently stable for direct charge recombination and generation of their lowest energy exciton (emissive) states.[16,17] Spectroelectrochemical techniques have also been used to study electron injection and bleaching of the lowest energy exciton absorption bands in multilayer films of II−VI nanocrystalline materials, yielding estimates for first-reduction potentials and E_{CB}.[18−23]

Potential-modulated attenuated total reflectance (PM-ATR) spectroelectrochemistry on an electroactive waveguide platform (Figure 1), a form of electroreflectance spectroscopy,[24−26] provides the sensitivity to characterize redox potentials and rates of electron transfer (ET) for thin films of biomolecules, conducting polymers and charge-transfer salts at submonolayer surface coverages.[27,28] Monitoring electrochemically generated optical changes in the redox-active monolayer allows clear differentiation of Faradaic versus non-Faradaic events. We show here that PM-ATR enables, for the first time, characterization of *reversible* electron injection into submonolayer coverages of surface-tethered, pyridine-capped CdSe nanocrystals (pyr-CdSe NCs). Low surface coverages of pyr-CdSe NCs may reduce NC−NC interactions, but the redox processes of such thin and weakly absorbing films can only be characterized by a technique with the sensitivity of waveguide-based spectroelectrochemistry.[29−32] We anticipate that waveguide spectroelectrochemistry will allow systematic examination of the effects of capping ligand, electrolyte environment, and interparticle interactions on frontier orbital energies and rates of ET of semiconductor NCs films, which are critical parameters in designing new energy conversion materials.[1−6,8,10,14,19,21−23,33−35]

CdSe NCs (ca. 5 nm diameter), capped with mixed trioctylphosphine oxide/hexadecylamine (TOPO)/HDA) ligands, were prepared using the synthetic protocols detailed in the Supporting Information (SI).[4,36,37] After precipitation (3×) to remove excess ligand, capping ligands were displaced from the NCs in neat pyridine solutions. The

Received Date: April 12, 2010
Accepted Date: May 25, 2010

DOI: 10.1021/jz100475j | *J. Phys. Chem. Lett.* **2010**, *1*, 1900–1905

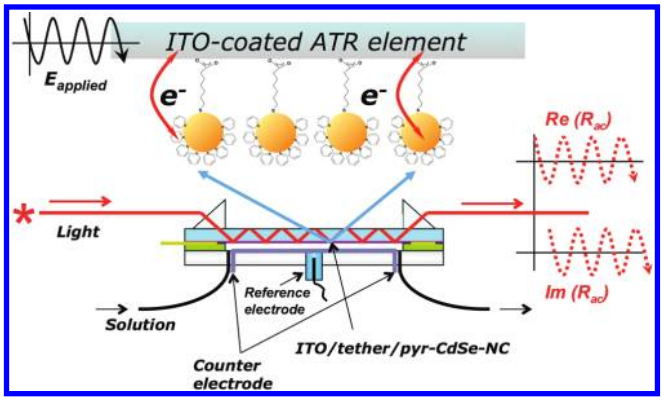

Figure 1. Schematic view of PM-ATR spectroelectrochemistry for monolayer-tethered NCs. Light is prism-coupled into and out of an ITO-coated waveguide, with pyr-CdSe NCs chemisorbed at the electrode/solution interface. The ITO electrode potential is modulated ±50 mV about −1.47 V vs Fc/Fc^+, which is the midpoint potential ($E_{applied}$) for reversible electron injection into the tethered NCs. The real (*Re*) and imaginary (*Im*) components of the ac portion of the electroreflectance response (R_{ac}) are monitored as a function of the modulation frequency, which is varied from 0.1 Hz to 1 kHz.

resultant pyr-CdSe NCs were precipitated using hexanes, washed, and dried.

Planar indium−tin oxide (ITO) electrodes, consisting of a 100 nm thick ITO layer coated on 1 mm thick soda lime glass (Colorado Concept Coatings, LLC), were used as planar waveguides.[32,38] ITO electrodes were first acid-activated,[39−41] and then modified with 3-mercaptopropionic acid (3-MPA), 6-mercaptohexanoic acid (6-MHA), or 11-mercaptoundecanoic acid (11-MUA) (see SI for details of the cleaning and modification procedure). NCs were deposited by immersing electrodes in 1 μM pyr-CdSe NC solutions (1:10 v/v pyridine/methanol) for periods up to 1 h (along with unmodified ITO as a control). Previous studies of adsorption of mercaptoalkylcarboxylic acids to ITO have shown that the carboxy groups are bound to the oxide surface,[42] leaving the terminal thiols available for subsequent capture of the pyr-CdSe NCs.[43]

ATR spectroscopy was used to monitor the adsorption of pyr-CdSe NCs to modified ITO electrodes using instrumentation similar to that described previously[32] (except that, in these experiments, a tungsten lamp was used as the source). Spectra were acquired every 2−3 min for 45 min after introduction of the pyr-CdSe NC solution to the ATR flow cell (see representative spectra in Figure 2a). The expected increase in absorbance for the lowest energy exciton band of 5 nm CdSe NCs was observed, with $\lambda_{max} \approx 609$ nm. A representative uptake curve on 3-MPA-modified ITO is shown in Figure 2b. Limiting coverages at this NC solution concentration are reached in ca. 20 min. Similar results were obtained for NCs adsorbed to 6-MHA- and 11-MUA-modified ITO. On the basis of these results, in subsequent experiments ITO electrodes were incubated for ca. 30 min for each NC deposition, to form the thin films that were the subject of the spectroelectrochemical studies described below.

Surface coverages of adsorbed pyr-CdSe NCs were estimated from the ATR spectra. After NC adsorption reached saturation on each type of electrode, the ATR flow cell was

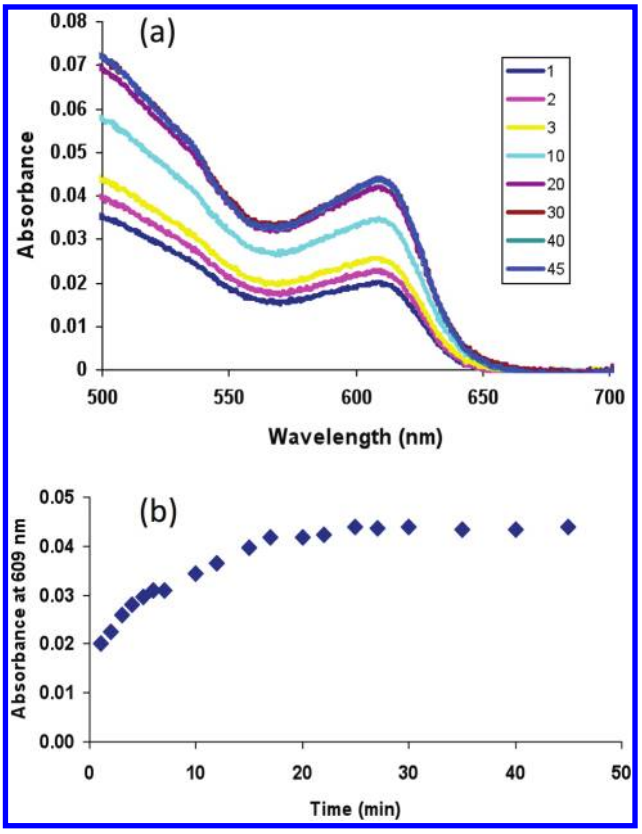

Figure 2. (a) Representative ATR spectra acquired during adsorption of pyr-CdSe NCs from a 1 μM solution to 3-MPA-modified ITO. The legend indicates the time (in minutes) at which the spectra were acquired. The spectra are normalized to absorbance values at 700 nm where there is no spectral response from CdSe NCs. (b) Absorbance (λ = 609 nm) versus exposure time to the pyr-CdSe NC solution; limiting coverages, corresponding to 10−20% of a monolayer (see text), were reached in under 30 min.

flushed with the electrolyte (0.1 M tetrabutyl ammonium perchlorate in acetonitrile (ACN)) that was used for the spectroelectrochemical measurements. An ATR spectrum was then acquired. The measured absorbance, A_f, is related to the surface coverage, Γ, by

$$\Gamma = A_f \cdot [1000N \cdot \varepsilon_f \cdot (I_e/I_i)]^{-1} \quad (1)$$

where N is the number of internal reflections at the interface between the ATR element and the sample (N = 10 in these experiments), and ε_f is the estimated molar absorptivity.[44] A value of 430 000 cm^{-1} M^{-1} for ε_f was estimated from the absorbance spectrum of dissolved 5 nm CdSe NCs using the empirical approach of Yu et al.[36] The term (I_e/I_i) is the evanescent transmitted interfacial intensity per unit incident intensity; it was calculated using a two-phase (glass/ACN) approximation as previously described.[30,44] In these experiments, the angle of internal reflection (θ) was ~65° and the refractive indices used for glass and ACN were 1.51 and 1.34, respectively.

Estimated Γ values for pyr-CdSe NCs adsorbed on 3-MPA-, 6-MHA-, and 11-MUA-modified ITO were near 10^{-12} mol/cm^2 (Table 1), which is approximately 10−20% of a close-packed monolayer, with an average NC−NC separation distance of

DOI: 10.1021/jz100475j | J. Phys. Chem. Lett. 2010, 1, 1900–1905

Table 1. Surface Coverage (Γ), Cell Series Resistance (R_S), Double Layer Capacitance (C_{dl}), and Electron Injection Rate Constants (k_S) for pyr-CdSe Films Adsorbed to Modified ITO Electrodes

	3-MPA/ITO	6-MHA/ITO	11-MUA/ITO
Γ (mol/cm^2) [a]	1.3×10^{-12}	1.8×10^{-12}	0.8×10^{-12}
R_S ($\Omega \cdot$cm^2) [b]	75 ± 3 ($n = 3$)	55 ($n = 2$)	72 ± 9 ($n = 4$)
C_{dl} (μF/cm^2) [b]	22 ± 1 ($n = 3$)	21 ($n = 2$)	15.0 ± 0.4 ($n = 4$)
k_S (s^{-1}) [c]	650 ± 230 ($n = 6$)	530 ± 32 ($n = 3$)	530 ± 38 ($n = 3$)

[a] Surface coverages were estimated from ATR spectroscopy (eq 1) as described in the text. [b] The electrochemical cell parameters R_s and C_{dl} were determined by electrochemical impedance spectroscopy.[24,25,27,28,50] [c] Rate constants were calculated from $k_s = 0.5\omega^2 R_S C_{dl}$, where ω is the modulation frequency at which the real component of the reflectance signal is zero.[24,25,27,28,50]

ca. three NC diameters (10−15 nm). Absorbance values at $\lambda_{max} \approx 609$ nm are ca. 0.1 A.U. at these coverages, which suggests that the limit of detection (LOD) with the conventional ATR platform used here is ca. 1% of a monolayer. The LOD would be substantially lower using a much thinner, single-mode waveguide platform, where the equivalent number of internal reflections exceeds 1000 per cm along the beam propagation axis in the waveguide.[29,45] On unmodified ITO surfaces, pyr-CdSe NCs adsorbed weakly relative to modified ITO, with saturation coverages of ca. 10^{-13} mol/cm^2.

Figure 3 shows field-emission scanning electron microscopy (FE-SEM) images of an unmodified ITO electrode and 3-MPA -and 6-MHA-modified ITO to which pyr-CdSe NCs have been adsorbed. Just a few NCs can be imaged on the unmodified ITO electrode. Relatively larger numbers of apparently isolated NCs and small clusters of NCs are visible on the 3-MPA- and 6-MHA-modified electrodes. The NCs appear to be mainly concentrated along grain boundaries in the ITO surface. They are spaced farther apart on average relative to the spacing expected based on the Γ values in Table 1, but this difference is not unexpected. Counting adsorbed NCs in these SEM images will likely lead to an underestimate of the actual surface coverage because (a) it is difficult to determine the number of NCs in clusters and (b) the rough ITO surface morphology and the tendency of NCs to localize in/along grain boundaries makes it probable that less than 100% of the adsorbed NCs are imaged.

On unmodified (bare) ITO surfaces, the spectroelectrochemical responses of adsorbed pyr-CdSe NCs were difficult to detect. In contrast, for NCs tethered to 3-MPA-, 6-MHA-, and 11-MUA-modified electrodes, complete and reversible bleaching of the lowest energy exciton absorption band (1S →1P transition) was observed at potentials estimated to be sufficient to inject electrons into the NC conduction band (Figure 4A).[15,20,21] The midpoint potential for the bleaching process was observed at −1.47 V versus ferrocene/ferrocenium (Fc/Fc^+) with complete bleaching at −1.75 V, and these values were invariant with tether length. The optical gap of 5 nm CdSe NCs, ∼2.04 eV, was calculated[36] from the λ_{max} of 609 nm. From the onset potentials for reduction and correction of the reference electrode to the vacuum scale,[46] E_{CB} and E_{VB} were estimated to be −3.5 eV and −5.5 eV, respectively.

These energy levels are consistent with values estimated from solution and thin film voltammetric and spectroelectrochemical studies of CdSe NCs.[7,15,20,21] However, they are smaller (i.e., the energies are closer to the vacuum level) by ca. 0.8−1 eV versus E_{CB} and E_{VB} values estimated from UV photoemission studies of surface-confined CdSe NCs (and corrected for shifts in local vacuum level).[9,43,47] Differences in the frontier orbital energy levels between vacuum and electrolyte environments have been predicted by Brus and coworkers, resulting from polarization effects in the NC and differences in the dielectric constants of electrolyte versus vacuum environments.[35,48] Resolving the apparent differences in these frontier orbital energies will be important in future studies using these NCs as either photocatalysts, or as donors or acceptors in photovoltaic platforms, since these energies determine the driving force for ET reactions to host polymers, host oxides, and/or to solution electron acceptors or donors.[1−3,5,9]

In the PM-ATR experiments, a 610 nm bandpass filter (∼17 nm fwhm) was placed between the ATR cell and photomultiplier tube detector to control the spectral bandwidth. The potential applied to the pyr-CdSe NC/tether/ITO electrode was modulated (±50 mV) about a midpoint potential ($E_{applied}$) of −1.47 V versus Fc/Fc^+. The real and imaginary reflectance components were measured over a modulation frequency range of 0.1 Hz to 1 kHz (Figure 4B). The frequency, ω, at which the real component of the reflectance signal is zero, coupled with measurements of the series (uncompensated) resistance, R_S, and double layer capacitance, C_{dl}, leads to an estimate for the apparent rate constant (k_S) for the reversible electron injection/bleaching in the NC film.[27,28] R_S, C_{dl}, and k_S values are listed in Table 1 for pyr-CdSe NCs tethered on 3-MPA-, 6-MHA-, and 11-MUA-modified electrodes. The apparent rate constants are ca. 500 s^{-1} and show no dependence on tether length.

These rate constants are greater than previous measurements on films of small molecules and metalloproteins linked or absorbed to ITO, but less than that of thiophene-based conducting polymers grown electrochemically from ITO.[27,28,49−52] We have recently shown that ITO electrodes such as those used here, modified or unmodified, are electrochemically active only at small fractions of their geometric area, and this results in relatively low rates of ET for a variety of dissolved and adsorbed molecules and conducting polymers.[27,39,40,49,53,54] Here we observe nearly quantitative and fully reversible bleaching of the lowest energy excitonic absorbance band of adsorbed NCs, which shows that the fraction of the NC film that is electroactive is near unity. It is unlikely, however, that NCs adsorb only to electrochemically active regions of the ITO surface. Given that k_S does not depend on tether length, we hypothesize that electron injection into a subpopulation of the adsorbed NCs occurs at

DOI: 10.1021/jz100475j | J. Phys. Chem. Lett. 2010, 1, 1900–1905

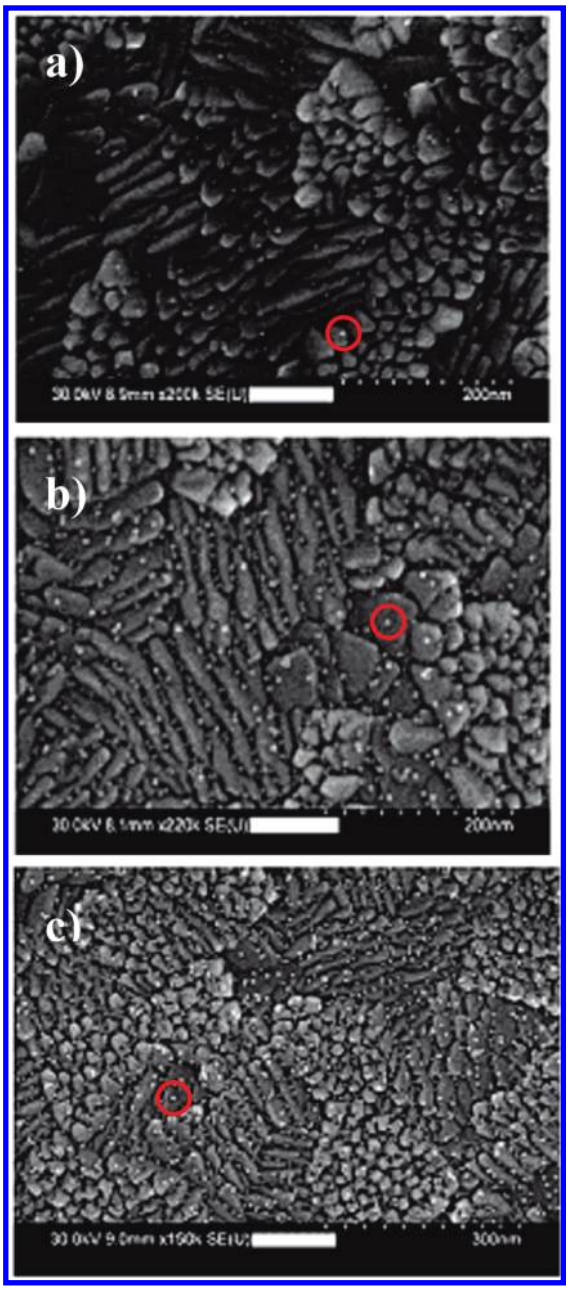

Figure 3. Representative FE-SEM images of pyr-CdSe NCs adsorbed to different ITO surfaces: (a) on bare ITO; (b) on 3-MPA-modified ITO; (c) on 6-MHA-modified ITO. In panels a and b, the scale bar = 200 nm; in panel c, the scale bar = 300 nm. Isolated NCs and small clusters of NCs are observable (examples are circled in red). Additional images are shown in the SI.

high rates at a limited number of electroactive sites (i.e., "hot spots") on the heterogeneous ITO surface, and at much reduced rates elsewhere, owing to the barriers that exist at the electrode surface toward charge injection.[40] Self-exchange between adjacent NCs is also possible, but given the low NC surface coverages used in this study, these self-exchange rates are likely to be quite low.

Waveguide ATR spectroelectrochemistry is a relatively easily implemented technology that enables two important

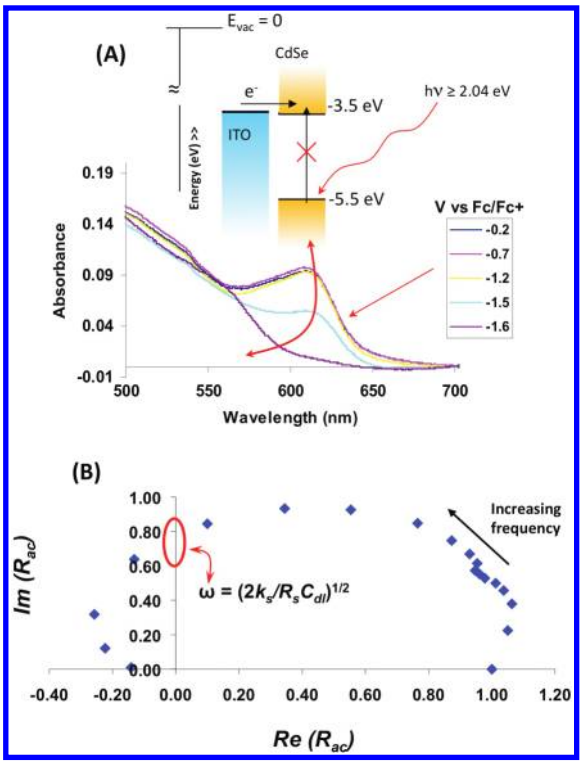

Figure 4. (A) Representative ATR spectra obtained for a submonolayer film of 5 nm pyr-CdSe NCs adsorbed on 3-MPA-modified ITO, immersed in electrolyte, as a function of applied potential. The 1S→1P absorption band is reversibly bleached at a midpoint potential of −1.47 V vs Fc/Fc^+ (−1.1 V vs normal hydrogen electrode (NHE)). Above the spectra is a schematic view of estimated frontier orbital energies of these 5.0 nm NCs with respect to vacuum (assumed value for NHE = −4.6 eV[46]). (B) Plot of normalized values of imaginary (*Im* (R_{ac})) vs real (*Re* (R_{ac})) reflectance components measured in a PM-ATR experiment for pyr-CdSe NCs adsorbed to 3-MPA-modified ITO. Example data for 6-MHA- and 11-MUA-modified ITO are presented in the SI. The normalized values were calculated as described previously,[27,28] and the curve was fit to a polynomial function to determine the frequency (ω) at which *Re* (R_{ac}) is zero (indicated by the red ellipse). In conjunction with the cell series resistance (R_S) and the double-layer capacitance (C_{dl}), determined from impedance experiments, ω was used to calculate the rate constant (k_s) for reversible electron injection into the tethered NCs (data listed in Table 1).

types of future experiments: (i) For CdSe and related semiconductor NCs that can be reduced in solution environments, we will be able to easily estimate first-reduction potentials and E_{CB}, for both low and high coverage NC films and as a function of NC diameter. Different solvents and dipolar capping ligands may change frontier orbital energies and/or local vacuum levels, and we anticipate good sensitivity for quantification of these changes, down to ca. ± 50 meV. Waveguide spectroelectrochemistry allows the characterization of these electron injection processes under conditions that ensure that they are chemically reversible, something that has not been observed in previous solution or voltammetric studies.[15−22] (ii) Switching rates for these electron injection processes can be measured using potential-modulated waveguide ATR. We anticipate that PM-ATR will enable characterization of the dynamics of electrochemical processes for a wide range of nanocrystalline materials, as bare NCs, or surrounded by

DOI: 10.1021/jz100475j | J. Phys. Chem. Lett. 2010, 1, 1900–1905

ultrathin polymer, oxide, or electrolyte hosts, or electrolyte environments of variable dielectric strength.

SUPPORTING INFORMATION AVAILABLE Experimental procedures for the preparation of pyr-CdSe NCs and modification of ITO with mercaptoalkylcarboxylic acids, higher resolution FE-SEM images of pyr-CdSe NCs adsorbed to bare and modified ITO, and PM-ATR data for 6-MHA and 11-MUA. This material is available free of charge via the Internet at http://pubs.acs.org.

AUTHOR INFORMATION

Corresponding Author:

*To whom correspondence should be addressed. E-mail: nra@email.arizona.edu (N.R.A.); saavedra@email.arizona.edu (S.S.S.).

Present Addresses:

† Institut für Physikalische Chemie, Universität zu Köln, Luxemburger Str. 116, D-50939 Köln.

ACKNOWLEDGMENT S.S.S. and N.R.A. gratefully acknowledge support from the Division of Chemical Sciences, Geosciences, and Biosciences, Office of Basic Energy Sciences of the U.S. Department of Energy through Grant DE-FG03-02ER15753 and the Center for Interface Science: Solar-Electric Materials (CIS:SEM), an Energy Frontier Research Center funded by the U.S. Department of Energy, Office of Basic Energy Sciences, under Award Number DE-SC0001084, for the majority of the personnel funding for this project. We also acknowledge grants from the National Science Foundation (CHE-0517963 (N.R.A.) and CHE-0518702 (S.S.S.)) for support of some of the critical instrumentation used here. The Arizona Board of Regents TRIF program — Arizona Research Institute for Solar Energy (AzRISE) provided partial research support for Z.O.A. Z.O.A. also gratefully acknowledges partial support from a fellowship from Merck Research Laboratories.

REFERENCES

(1) Harris, C.; Kamat, P. V. Photocatalysis with CdSe Nanoparticles in Confined Media: Mapping Charge Transfer Events in the Subpicosecond to Second Timescales. *ACS Nano* **2009,** *3*, 682–690.

(2) Farrow, B.; Kamat, P. V. CdSe Quantum Dot Sensitized Solar Cells. Shuttling Electrons through Stacked Carbon Nanocups. *J. Am. Chem. Soc.* **2009,** *131*, 11124–11131.

(3) Kongkanand, A.; Tvrdy, K.; Takechi, K.; Kuno, M.; Kamat, P. V. Quantum Dot Solar Cells. Tuning Photoresponse through Size and Shape Control of CdSe−TiO_2 Architecture. *J. Am. Chem. Soc.* **2008,** *130*, 4007–4015.

(4) Shallcross, R. C.; D'Ambruoso, G. D.; Korth, B. D.; Hall, H. K.; Zheng, Z. P.; Pyun, J.; Armstrong, N. R. Poly(3,4-ethylenedioxythiophene) - Semiconductor Nanoparticle Composite Thin Films Tethered to Indium Tin Oxide Substrates Via Electropolymerization. *J. Am. Chem. Soc.* **2007,** *129*, 11310–11311.

(5) Shallcross, R. C.; D'Ambruoso, G. D.; Pyun, J.; Armstrong, N. R. Photoelectrochemical Processes in Polymer-Tethered CdSe Nanocrystals. *J. Am. Chem. Soc.* **2010,** *132*, 2622–2632.

(6) Kamat, P. V. Meeting the Clean Energy Demand: Nanostructure Architectures for Solar Energy Conversion. *J. Phys. Chem. C* **2007,** *111*, 2834–2860.

(7) Markus, T. Z.; Wu, M.; Wang, L.; Waldeck, D. H.; Oron, D.; Naaman, R. Electronic Structure of CdSe Nanoparticles Adsorbed on Au Electrodes by an Organic Linker: Fermi Level Pinning of the HOMO. *J. Phys. Chem. C* **2009,** *113*, 14200–14206.

(8) Agrios, A. G.; Cesar, I.; Comte, P.; Nazeeruddin, M. K.; Gratzel, M. Nanostructured Composite Films for Dye-Sensitized Solar Cells by Electrostatic Layer-by-Layer Deposition. *Chem. Mater.* **2006,** *18*, 5395–5397.

(9) Carlson, B.; Leschkies, K.; Aydil, E. S.; Zhu, X. Y. Valence Band Alignment at Cadmium Selenide Quantum Dot and Zinc Oxide (1010) Interfaces. *J. Phys. Chem. C* **2008,** *112*, 8419–8423.

(10) Niu, Y. H.; Munro, A. M.; Cheng, Y. J.; Tian, Y. Q.; Liu, M. S.; Zhao, J. L.; Bardecker, J. A.; Plante, I. J. L.; Ginger, D. S.; Jen, A. K. Y. Improved Performance from Multilayer Quantum Dot Light-Emitting Diodes via Thermal Annealing of the Quantum Dot Layer. *Adv. Mater.* **2007,** *19*, 3371–3376.

(11) Campbell, I. H.; Crone, B. K. Efficient, Visible Organic Light-Emitting Diodes Utilizing a Single Polymer Layer Doped with Quantum Dots. *Appl. Phys. Lett.* **2008,** *92*, 043303.

(12) Huynh, W. U.; Dittmer, J. J.; Libby, W. C.; Whiting, G. L.; Alivisatos, A. P. Controlling the Morphology of Nanocrystal-Polymer Composites for Solar Cells. *Adv. Funct. Mater.* **2003,** *13*, 73–79.

(13) Huynh, W. U.; Dittmer, J. J.; Alivisatos, A. P. Hybrid Nanorod-Polymer Solar Cells. *Science* **2002,** *295*, 2425–2427.

(14) Huynh, W. U.; Dittmer, J. J.; Teclemariam, N.; Milliron, D. J.; Alivisatos, A. P.; Barnham, K. W. J. Charge Transport in Hybrid Nanorod−Polymer Composite Photovoltaic Cells. *Phys. Rev. B* **2003,** *67*, 115326.

(15) Inamdar, S. N.; Ingole, P. P.; Haram, S. K. Determination of Band Structure Parameters and the Quasi-Particle Gap of CdSe Quantum Dots by Cyclic Voltammetry. *ChemPhysChem* **2008,** *9*, 2574–2579.

(16) Bae, Y.; Myung, N.; Bard, A. J. Electrochemistry and Electrogenerated Chemiluminescence of CdTe Nanoparticles. *Nano Lett.* **2004,** *4*, 1153–1161.

(17) Myung, N.; Ding, Z. F.; Bard, A. J. Electrogenerated Chemiluminescence of CdSe Nanocrystals. *Nano Lett.* **2002,** *2*, 1315–1319.

(18) Haram, S. K.; Quinn, B. M.; Bard, A. J. Electrochemistry of CdS Nanoparticles: A Correlation between Optical and Electrochemical Band Gaps. *J. Am. Chem. Soc.* **2001,** *123*, 8860–8861.

(19) Guyot-Sionnest, P. Charging Colloidal Quantum Dots by Electrochemistry. *Microchim. Acta* **2008,** *160*, 309–314.

(20) Wang, C. J.; Shim, M.; Guyot-Sionnest, P. Electrochromic Nanocrystal Quantum Dots. *Science* **2001,** *291*, 2390–2392.

(21) Guyot-Sionnest, P.; Wang, C. Fast Voltammetric and Electrochromic Response of Semiconductor Nanocrystal Thin Films. *J. Phys. Chem. B* **2003,** *107*, 7355–7359.

(22) Wehrenberg, B. L.; Guyot-Sionnest, P. Electron and Hole Injection in PbSe Quantum Dot Films. *J. Am. Chem. Soc.* **2003,** *125*, 7806–7807.

(23) Wang, C. J.; Shim, M.; Guyot-Sionnest, P. Electrochromic Semiconductor Nanocrystal Films. *Appl. Phys. Lett.* **2002,** *80*, 4–6.

(24) Feng, Z. Q.; Imabayashi, S.; Kakiuchi, T.; Niki, K. Determination of the Electrode Kinetic Parameters of a Species Immobilized on Electrodes Using the Electroreflectance (ER) Voltammogram. *J. Electroanal. Chem.* **1996,** *408*, 15–20.

(25) Feng, Z. Q.; Sagara, T.; Niki, K. Application of Potential-Modulated UV-Visible Reflectance Spectroscopy to Electron-Transfer Rate Measurements for Adsorbed Species on Electrode Surfaces. *Anal. Chem.* **1995,** *67*, 3564–3570.

(26) Nagatani, H.; Sagara, T. Potential-Modulation Spectroscopy at Solid/Liquid and Liquid/Liquid Interfaces. *Anal. Sci.* **2007,** *23*, 1041–1048.

DOI: 10.1021/jz100475j | *J. Phys. Chem. Lett.* **2010,** *1*, 1900–1905

(27) Araci, Z. O.; Runge, A. F.; Doherty, W. J.; Saavedra, S. S. Correlating Molecular Orientation Distributions and Electrochemical Kinetics in Subpopulations of an Immobilized Protein Film. *J. Am. Chem. Soc.* **2008,** *130*, 1572–1573.

(28) Doherty, W. J., III; Wysocki, R. J.; Armstrong, N. R.; Saavedra, S. S. Potential-Modulated, Attenuated Total Reflectance Spectroscopy of Poly(3,4-Ethylenedioxythiophene) and Poly(3,4-ethylenedioxythiophene methanol) Copolymer Films on Indium−Tin Oxide. *J. Phys. Chem. B* **2006,** *110*, 4900–4907.

(29) Bradshaw, J. T.; Mendes, S. B.; Saavedra, S. S. Planar Integrated Optical Waveguide Spectroscopy. *Anal. Chem.* **2005,** *77*, 28A–36A.

(30) Saavedra, S. S.; Reichert, W. M. Integrated Optical Attenuated Total Reflection Spectrometry of Aqueous Superstrates Using Prism-Coupled Polymer Waveguides. *Anal. Chem.* **1990,** *62*, 2251–2256.

(31) Bradshaw, J. T.; Mendes, S. B.; Armstrong, N. R.; Saavedra, S. S. Broadband Coupling into a Single-Mode, Electroactive Integrated Optical Waveguide for Spectroelectrochemical Analysis of Surface-Confined Redox Couples. *Anal. Chem.* **2003,** *75*, 1080–1088.

(32) Doherty, W. J.; Donley, C. L.; Armstrong, N. R.; Saavedra, S. S. Broadband Spectroelectrochemical Attenuated Total Reflectance Instrument for Molecular Adlayer Studies. *Appl. Spectrosc.* **2002,** *56*, 920.

(33) Hodes, G. Comparison of Dye- and Semiconductor-Sensitized Porous Nanocrystalline Liquid Junction Solar Cells. *J. Phys. Chem. C* **2008,** *112*, 17778–17787.

(34) Campbell, I. H.; Crone, B. K. Efficient, Visible Organic Light-Emitting Diodes Utilizing a Single Polymer Layer Doped with Quantum Dots. *Appl. Phys. Lett.* **2008,** *92*, 043303.

(35) Rabani, E.; Hetenyi, B.; Berne, B. J.; Brus, L. E. Electronic Properties of CdSe Nanocrystals in the Absence and Presence of a Dielectric Medium. *J. Chem. Phys.* **1999,** *110*, 5355–5369.

(36) Yu, W. W.; Qu, L. H.; Guo, W. Z.; Peng, X. G. Experimental Determination of the Extinction Coefficient of CdTe, CdSe, and CdS Nanocrystals. *Chem. Mater.* **2003,** *15*, 2854–2860.

(37) Qu, L. H.; Peng, X. G. Control of Photoluminescence Properties of CdSe Nanocrystals in Growth. *J. Am. Chem. Soc.* **2002,** *124*, 2049–2055.

(38) Runge, A. F.; Mendes, S. B.; Saavedra, S. S. Order Parameters and Orientation Distributions of Solution Adsorbed and Microcontact Printed Cytochrome *c* Protein Films on Glass and ITO. *J. Phys. Chem. B* **2006,** *110*, 6732–6739.

(39) Brumbach, M.; Veneman, P. A.; Marrikar, F. S.; Schulmeyer, T.; Simmonds, A.; Xia, W.; Lee, P.; Armstrong, N. R. Surface Composition and Electrical and Electrochemical Properties of Freshly Deposited and Acid-Etched Indium Tin Oxide Electrodes. *Langmuir* **2007,** *23*, 11089–11099.

(40) Armstrong, N. R.; Veneman, P. A.; Ratcliff, E. M.; Placencia, D.; Brumbach, M. Oxide Contacts in Organic Photovoltaics: Characterization and Control of Near-Surface Composition in Indium−Tin Oxide (ITO) Electrodes. *Acc. Chem. Res.* **2009,** *42*, 1748–1757.

(41) Ratcliff, E. L.; Lee, P. A.; Armstrong, N. R. Work Function Control of Hole-Selective Polymer/ITO Anode Contacts: An Electrochemical Doping Study. *J. Mater. Chem.* **2010,** *20*, 2672–2679.

(42) Yan, C.; Zharnikov, M.; Golzhauser, A.; Grunze, M. Preparation and Characterization of Self-Assembled Monolayers on Indium Tin Oxide. *Langmuir* **2000,** *16*, 6208–6215.

(43) Munro, A. M.; Zacher, B.; Armstrong, N. R. Photoemission Spectroscopy of Tethered CdSe Nanocrystals: Ionization Potentials and Local Vacuum Levels as a Function of Capping Ligand. *ACS Appl. Mater. Interfaces* **2010,** *2*, 863–869.

(44) Saavedra, S. S.; Reichert, W. M. In Situ Quantitation of Protein Adsorption Density by Integrated Optical Waveguide ATR Spectrometry. *Langmuir* **1991,** *7*, 995–999.

(45) Skrdla, P. J.; Saavedra, S. S.; Armstrong, N. R.; Mendes, S. B.; Peyghambarian, N. Sol-Gel-Based, Planar Waveguide Sensor for Water Vapor. *Anal. Chem.* **1999,** *71*, 1332–1337.

(46) Kelly, C. P.; Cramer, C. J.; Truhlar, D. G. Single-Ion Solvation Free Energies and the Normal Hydrogen Electrode Potential in Methanol, Acetonitrile, and Dimethyl Sulfoxide. *J. Phys. Chem. B* **2007,** *111*, 408–422.

(47) Colvin, V. L.; Alivisatos, A. P.; Tobin, J. G. Valence-Band Photoemission from a Quantum-Dot System. *Phys. Rev. Lett.* **1991,** *66*, 2786–2789.

(48) Brus, L. E. A Simple-Model for the Ionization-Potential, Electron-Affinity, and Aqueous Redox Potentials of Small Semiconductor Crystallites. *J. Chem. Phys.* **1983,** *79*, 5566–5571.

(49) Donley, C.; Dunphy, D.; Paine, D.; Carter, C.; Nebesny, K.; Lee, P.; Alloway, D.; Armstrong, N. R. Characterization of Indium-Tin Oxide Interfaces Using X-Ray Photoelectron Spectroscopy and Redox Processes of a Chemisorbed Probe Molecule: Effect of Surface Pretreatment Conditions. *Langmuir* **2002,** *18*, 450–457.

(50) Araci, Z. O.; Runge, A. F.; Doherty, W. J., III; Saavedra, S. S. Potential-Modulated Attenuated Total Reflectance Spectroscopy of Prussian Blue Films on ITO. *Israel J. Chem.* **2006,** *46*, 249–255.

(51) El Kasmi, A.; Leopold, M. C.; Galligan, R.; Robertson, R. T.; Saavedra, S. S.; El Kacemi, K.; Bowden, E. F. Adsorptive Immobilization of Cytochrome *c* on Indium/Tin Oxide (ITO): Electrochemical Evidence for Electron Transfer Induced Conformational Changes. *Electrochem. Commun.* **2002,** *4*, 177–181.

(52) Runge, A. F.; Saavedra, S. S. Comparison of Microcontact-Printed and Solution-Adsorbed Cytochrome *c* Films on Indium Tin Oxide Electrodes. *Langmuir* **2003,** *19*, 9418–9424.

(53) Carter, C.; Brumbach, M.; Donley, C.; Hreha, R. D.; Marder, S. R.; Domercq, B.; Yoo, S.; Kippelen, B.; Armstrong, N. R. Small Molecule Chemisorption on Indium-Tin Oxide Surfaces: Enhancing Probe Molecule Electron-Transfer Rates and the Performance of Organic Light-Emitting Diodes. *J. Phys. Chem. B* **2006,** *110*, 25191–25202.

(54) Marrikar, F. S.; Brumbach, M.; Evans, D. H.; Lebron-Paler, A.; Pemberton, J. E.; Wysocki, R. J.; Armstrong, N. R. Modification of Indium-Tin Oxide Electrodes with Thiophene Copolymer Thin Films: Optimizing Electron Transfer to Solution Probe Molecules. *Langmuir* **2007,** *23*, 1530–1542.

DOI: 10.1021/jz100475j | *J. Phys. Chem. Lett.* **2010,** *1*, 1900–1905